Encoding calamitic mesomorphism in thermotropic lanthanidomesogens†

Emmanuel Terazzi,[a] Bernard Bocquet,[a] Stéphane Campidelli,[b] Bertrand Donnio,[c] Daniel Guillon,[c] Robert Deschenaux*[b] and Claude Piguet*[a]

Peripheral cyanobiphenyl dendrimers impose a microphase organization compatible with smectic mesomorphism, in which the bulky nine-coordinate lanthanide core is located between the decoupled mesogenic sublayers made up of parallel cyanobiphenyl groups.

The design of thermotropic metallomesogens (metal-containing liquid crystals)[1] follows similar rules as those applied for organic compounds, and a common strategy consists of designing anisometric molecules possessing at least two incompatible parts, which are separated by a molecular interface. The incompatible parts generally correspond to polarizable rigid cores and poorly polarizable flexible chains, the latter being located at the periphery of the molecule.[2] The existence of these two spatially separated portions is responsible for the generation of two successive phase transitions corresponding (i) to the melting of the aliphatic chains, and the concomitant formation of the liquid-crystalline phase, followed by (ii) the ultimate melting of residual packed rigid cores, which leads to the nematic phase or to the isotropic liquid.[2] For trivalent lanthanide metal ions, Ln^{III}, the considerable size of their high-coordination spheres limits the efficiency of the microsegregation processes operating between the polarizable bulky metallo-organic core and the appended flexible paraffinic chains, and the occurrence of thermotropic lanthanide-containing liquid crystals (lanthanidomesogens) remains rare.[3] Two main strategies have been considered for restoring the minimal electronic and structural incompatibilities required for an efficient microsegregation: (1) the Ln^{III} ions are embedded into aromatic polarizable cavities produced by several wrapped ligands, which globally display rodlike or disklike shapes (Fig. S1, ESI†),[3–5] or (2) the coordination of Ln^{III} to pro-mesogenic polycatenar ligands possessing curved molecular interfaces and large melting entropies helps to induce thermotropic mesomorphism at 'low' temperature,

as observed for [Ln(L1)(NO$_3$)$_3$] (Fig. 1).[6] An alternative strategy was reported for the design of [60]fullerene-containing liquid crystals, in which the bulky C$_{60}$ unit is embedded within a flexible part connecting two peripheral mesogenic dendritic cyanobiphenyl cores in L2 (Fig. 1).[7] Since the intermolecular interactions responsible for the residual organization of the rigid cores of L2 in the mesophase mainly result from the parallel arrangement of the mesogenic cyanobiphenyl groups, a smectic A phase was obtained. Based on this study, one can envisage replacing C$_{60}$ with other bulky edifices, such as lanthanide cores. Following this reasoning, we aim at forcing lanthanidomesogens to form fluid thermotropic smectic and nematic phases by using the low-generation dendritic complexes [Ln(Li)(NO$_3$)$_3$] (i = 3, 4), in which a central tridentate 2,6-bis(benzimidazole)pyridine unit replaces the malonate spacer found in L2 (Fig. 1). The recent report of nematic mesomorphism around 85–90 °C for the related, but unsymmetrical complexes [Ln(L5)(diketonate)$_3$], in which cyanobiphenyl groups are decoupled from the bulky lanthanide core, is an encouraging pioneering step towards the controlled formation of fluid layered organisation with luminescent lanthanides (Fig. 1).[8]
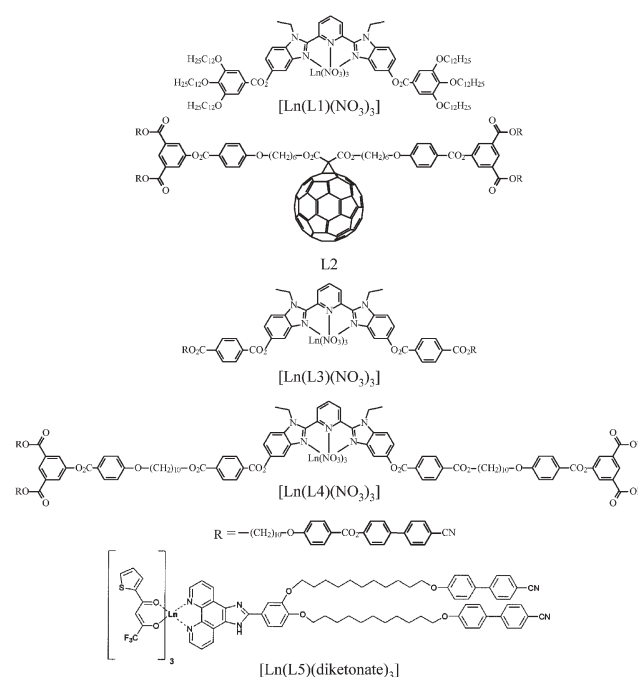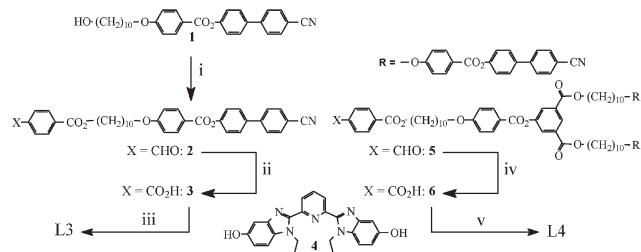
[a]Department of Inorganic, Analytical and Applied Chemistry, University of Geneva, 30 quai E. Ansermet, CH-1211 Geneva 4, Switzerland.
E-mail: Claude.Piguet@chiam.unige.ch.; Fax: +4122 379 6830;
Tel: +4122 379 6034
[b]Institut de Chimie, Université de Neuchâtel, Av. de Bellevaux 51, CP 158, CH-2009 Neuchâtel, Switzerland.
E-mail: robert.deschenaux@unine.ch
[c]Institut de Physique et Chimie des Matériaux de Strasbourg–IPCMS, Groupe des Matériaux Organiques, 23 rue du Loess, B.P. 43, F-67034 Strasbourg Cedex 2, France.

Fig. 1 Molecular structures of L2[7] and of the complexes [Ln(L1)(NO$_3$)$_3$],[6b] [Ln(Li)(NO$_3$)$_3$] (i = 3, 4), and [Ln(L5)(diketonate)$_3$].[8]

Scheme 1 Reagents: (i) CH_2Cl_2, DCC, 4-DMAP, 4-carboxybenzaldehyde, rt, 16 h, 33% (ii) THF, H_2O, $NaClO_2$, H_2NSO_3H, rt, 2 h, 97% (iii) CH_2Cl_2, EDCI, 4-DMAP, 12 h, reflux, 77% (iv) THF, H_2O, $NaClO_2$, H_2NSO_3H, rt, 2 h, 100% (v) CH_2Cl_2, EDCI, 4-DMAP, 12 h, reflux, 70%.

The syntheses of the ligands L3 and L4 are shown in Scheme 1. Esterification of **1**[7] with 4-carboxybenzaldehyde gives **2**, which is oxidized into the corresponding carboxylic acid **3**. A second esterification allows its coupling to the tridentate binding unit **4**[10] to give L3.‡ Ligand L4 was prepared in a similar way from the aldehyde derivative **5**.[9] The ^{1}H NMR spectra of L3 and L4 confirm dynamically-averaged C_{2v} symmetries on the NMR time scale, while the lack of NOE effect between the ethyl residues and the protons connected at the *meta*-positions of the pyridine ring agrees with the usual *trans–trans* arrangement of the non-coordinated 2,6-bis(benzimidazole)pyridine core (Figure S2a, ESI†).[6b]

Lanthanide complexes with formula [Ln(L*i*)(NO$_3$)$_3$]·xH$_2$O (i = 3, 4; ESI, Table S1†) are obtained by mixing stoichiometric amounts of the hydrated lanthanide salt Ln(NO$_3$)$_3$·nH$_2$O and L*i* in dichloromethane–acetonitrile (1 : 1). The presence of co-crystallized water molecules is confirmed by thermogravimetric (TG) measurements, which show dehydration of the complexes during the first heating process in the 25–100 °C range. In solution, the complexation of L4 can be followed by ^{1}H NMR and the diagnostic complexation shifts observed for the aromatic protons in the diamagnetic [Lu(L4)(NO$_3$)$_3$] complex (Fig. S2b and Table S2, ESI†) points to the dynamically-average C_{2v} meridional tri-coordination of the 2,6-bis(benzimidazol-2-yl)pyridine to the metal ion, as previously demonstrated for [Lu(L1)(NO$_3$)$_3$].[6b] The detection of NOE effects between the ethyl residues and the protons connected at the *meta*-positions of the pyridine ring confirms the *cis–cis* conformation of the coordinated tridentate receptor. The ^{1}H NMR spectra of the paramagnetic complexes [Eu(L4)(NO$_3$)$_3$] are different, not only because of the additional lanthanide-induced shifts (LIS) and lanthanide-induced relaxation (LIR) effects produced by the Eu-centred unpaired electrons, but also because each broadened resonance is split as the result of the dimerization process previously established for the closely related non-dendritic complex [Eu(L1)(NO$_3$)$_3$] (equilibrium (1) and Fig. S2c, ESI†).[6b]

$$2[Eu(L4)(NO_3)_3] \rightleftarrows [Eu_2(L4)_2(NO_3)_6] \quad K_d^{Eu,L4} \quad (1)$$
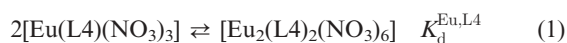
A DOSY experiment performed on [Eu(L4)(NO$_3$)$_3$] (CD$_2$Cl$_2$, 298 K) shows that a first series of peaks (series A in Fig. S2c ESI†) corresponds to a single species with an auto-diffusion coefficient $D_A = 2.7(1) \times 10^{-10}$ m^2 s^{-1}, while the second series of peaks (series B in Fig. S2c†) is assigned to a different species which diffuses slightly slower $D_B = 2.2(2) \times 10^{-10}$ m^2 s^{-1}. The ratio $D_A/D_B = 1.2(1)$ translates into MM$_B$/MM$_A$ = 1.8(2) by using eqn. (2),

in agreement with the dimerization process shown in equilibrium (1)[6b] (MM stands for the molecular mass of the complexes, $\bar{v}_A$ and $\bar{v}_B$ are the specific partial volumes).[11]

$$MM_B/MM_A = (D_A/D_B)^3 \cdot (\bar{v}_B/\bar{v}_A) \quad (2)$$

Integration of the variable-temperature ^{1}H NMR data shows the ratio [Eu(L4)(NO$_3$)$_3$]/[Eu$_2$(L4)$_2$(NO$_3$)$_6$] to smoothly increase from 5.9 at 298 K, to 20.0 at 318 K in CD$_2$Cl$_2$. Calculation of $K_d^{Eu,L4}$ (equilibrium (1)) at each temperature gives a linear van't Hoff plot, from which the thermodynamic parameters $\Delta H_d^{Eu,L4} = -55(4)$ kJ mol^{-1} and $\Delta S_d^{Eu,L4} = -166(11)$ J mol^{-1} K^{-1} can be determined (Fig. S3, ESI†). These parameters are typical for a dimerization process occurring in a non-coordinating solvent for Ln^{III} complexes (CD$_2$Cl$_2$), because the formation of the dimer is enthalpically driven (formation of two additional Eu–O bonds without breaking Eu-solvent bonds), but entropically limited (decrease of the translational entropy when two monomers dimerize). These values compare well with $\Delta H_d^{Eu,L1} = -54(4)$ kJ mol^{-1} and $\Delta S_d^{Eu,L1} = -162(16)$ J mol^{-1} K^{-1} previously reported for the nine-coordinated monomer [Eu(L1)(NO$_3$)$_3$],[6b] and this allows us to conclude that Eu^{III} is similarly nine-coordinated by the tridentate aromatic receptor ligand and three bidentate nitrates in [Eu(L4)(NO$_3$)$_3$] and in [Eu(L1)(NO$_3$)$_3$].

The thermal and liquid-crystalline properties of L3 and L4 were investigated by differential scanning calorimetry (DSC) and polarized transmitted light microscopy (PLM, Table 1). The nature of the phases was established from their optical textures (PLM), which display the typical Schlieren's texture of fluid nematic (N) phases. This strongly contrasts with the poorly fluid hexagonal columnar mesophase (Col$_h$) evidenced for the parent hexacatenar ligand L1, which confirms the beneficial effect of the peripheral cyanobiphenyl groups for inducing calamitic mesomorphism. Moreover, the reduced transition temperatures observed on going from L3 to L4 illustrate the favorable dendrimeric effect occurring in this system.[7,9] Examination of the

Table 1 Phase-transition temperatures and enthalpy and entropy changes for L3 and L4, and for the complexes [Ln(L4)(NO$_3$)$_3$] (Ln = Lu, Tb, Gd and Eu).

Compound	Transition[a]	T/°C	ΔH/ kJ mol^{-1}	ΔS/ J mol^{-1} K^{-1}
L3	G → N	82	—	—
	N → I[b]	324	—	—
L4	G → N	52	—	—
	N → I	238	11.0	21.5
[Lu(L4)(NO$_3$)$_3$]	G → SmA	100	—	—
	SmA → PCr[c]	150	—	—
	PCr → SmA	170		—
	SmA → I/Dec.	200	3.3	6.9
[Tb(L4)(NO$_3$)$_3$]	G → SmA	90	—	—
	SmA → I/Dec.	190	15.0	32.3
[Gd(L4)(NO$_3$)$_3$]	G → SmA	85	—	—
	SmA → I/Dec.	188	9.1	19.8
[Eu(L4)(NO$_3$)$_3$]	G → SmA	80	—	—
	SmA → I/Dec.	186	11.1	24.2

[a] G = glass, SmA = smectic A phase, N = nematic phase, I = isotropic fluid, Dec. = decomposition; temperatures are given as the onset of the peak observed during heating processes; the liquid-crystalline phases were identified from their optical textures and from XRD studies. [b] Too weak to be detected by DSC. [c] Re-entrant partially crystallized phase (PCr).
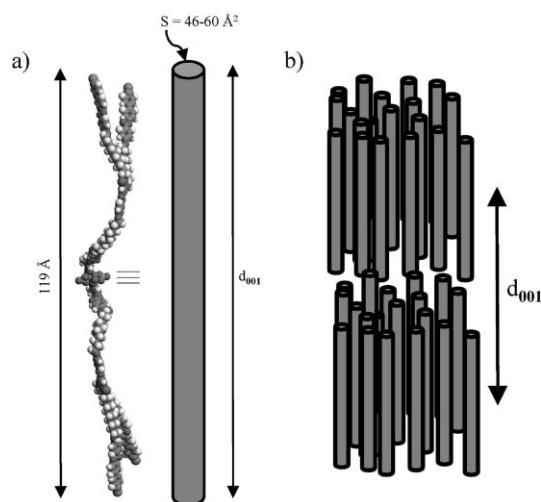
Fig. 2 (a) Simple molecular model for $[Ln(L4)(NO_3)_3]$ (Ln = Lu, Tb, Gd and Eu) in the unit cell. (b) Arrangement of $[Ln(L4)(NO_3)_3]$ in the SmA mesophase.

complexes by PLM indicates that only the complexes with L4 are mesogenic. Because of their reduced trend towards dimerization,[6b] only $[Ln(L4)(NO_3)_3]$ with metals of the second part of the lanthanide series (Ln = Eu, Gd, Tb and Lu) have been investigated by DSC (Fig. S4, ESI†) and small angle X-ray diffraction (SA-XRD) (Table S3 and Fig. S5, ESI †). The complexes are mesogenic over a large temperature range (Table 1), and PLM observations show fluid and birefringent textures. The phase transformation from the solid to the fluid phases usually corresponds to glass transitions (faint bend on the DSC traces), for which the temperatures have been determined by PLM. The isotropizations correspond to irreversible first-order phase transitions, because the complexes rapidly decompose in the liquid state at high temperature. Consequently, natural textures cannot form and the organization within the phases are deduced from small angle X-ray diffraction measurements collected during the first heating process. The X-ray diffraction patterns recorded for the mesogenic complexes $[Ln(L4)(NO_3)_3]$ (Ln = Eu, Gd and Tb) are similar. At 80–100 °C, two low-angle reflections start to develop, and reach maximum intensity at 160 °C, before breaking down at 180–200 °C. At 160 °C, two small-angle reflections in the ratio 1 : 2 were obtained, characteristic of a lamellar organization. They were indexed as the (00l) reflections of a smectic phase with $d_{001} \cong 120$ Å and $d_{002} \cong 60$ Å. (Table S3 and Fig. S5, ESI†). The additional diffuse band measured at larger angle ($d \cong 4.5$ Å) corresponds to the aliphatic molten chains. The behavior of $[Lu(L4)(NO_3)_3]$ is slightly different. Although the smectic phase starts to develop at 100 °C, an unspecified partially crystallized phase develops between 140 and 160 °C during the first heating event, which eventually restores the smectic phase at 190 °C.[6b] The large interlayer distances, assigned to the first harmonic of a smectic phase ($d_{001} \cong 120$ Å, Table S2, ESI†), agrees with the approximate 119 Å length estimated by a simple molecular modeling for a single complex $[Ln(L4)(NO_3)_3]$ in its extended conformation (Fig. 2a). In order to verify that the extended molecular conformation prevails in the mesophase, we determined the molecular area of such an arrangement in the smectic layers, and compared it to 44 Å², which accounts for the cross-section of

two parallel cyanobiphenyl segments corresponding to the termini of the extended rodlike complex (each segment occupies an average surface of 22 Å² in a SmA phase).[12] Taking an approximate, but realistic molecular density of $d = 1$ g cm^{-3} in the mesophase, we eventually estimated the molecular volume of the complex according to: $V = MM_{complex} \times \lambda \times 10^{-24}/d \times N_{av}$, ($MM_{complex}$, molecular weight of the complex, N_{av}, Avogadro's number, and λ, a temperature corrector, see ESI†) and then calculated the molecular area $A = V/d_{001}$.[13] We systematically found that $A \cong 46.0$–60 Å² (Table S3, ESI†), in agreement with an orthogonal arrangement of the terminal groups with respect to the layers, and thus to a SmA type of phase, reminiscent of that observed for some main-chain LC dendrimers (Fig. 2b).[13]

In conclusion, the typical columnar and cubic mesomorphism evidenced for the hexacatenar complexes $[Ln(L1)(NO_3)_3]$[6b] is replaced by smectogenic organization with the dendritic analogues $[Ln(L4)(NO_3)_3]$. These results are in line with previous observations reported for fullerene-containing liquid-crystalline dendrimers,[7,9,14] and larger decoupling between the mesogenic cyanobiphenyl groups and the polarizable lanthanide core, produced by the stepwise increase of the dendrimer generation, is a promising tool for further reducing melting temperatures, a crucial point for designing fluid calamitic lanthanidomesogens.

Notes and references

1 B. Donnio, D. Guillon, D. W. Bruce and R. Deschenaux, in *Comprehensive Coordination Chemistry II: From Biology to Nanotechnology*, ed. J. A. McCleverty and T. J. Meyer, Elsevier, Oxford, UK, 2003, vol. 7, ch. 7.9, pp. 357–627.

2 E. Terazzi, S. Suarez, S. Torelli, O. Mamula, H. Nozary, D. Imbert, J.-P. Rivera, E. Guillet, J.-M. Benech, G. Bernardinelli, R. Scopelliti, B. Donnio, D. Guillon, J.-C. G. Bünzli and C. Piguet, *Adv. Funct. Mater.*, 2006, 157 and references therein.

3 K. Binnemans and C. Görller-Walrand, *Chem. Rev.*, 2002, **102**, 2303.

4 (a) Y. G. Galyametdinov, G. I. Ivanova, A. V. Prosvirin and O. Kadkin, *Russ. Chem. Bull.*, 1994, **43**, 938; (b) K. Binnemans, Y. G. Galyametdinov, R. V. Deun, D. W. Bruce, S. R. Collinson, A. P. Polishchuk, I. Bikchantaev, W. Haase, A. V. Prosvirin, L. Tinchurina, I. Litvinov, A. Gubajdullin, A. Rakhmatullin, K. Uytterhoeven and L. V. Meervelt, *J. Am. Chem. Soc.*, 2000, **122**, 4335.

5 K. Binnemans, J. Sleven, S. D. Feyter, F. C. D. Schryver, B. Donnio and D. Guillon, *Chem. Mater.*, 2003, **15**, 3930 and references therein.

6 (a) K. Binnemans, K. Lodewyckx, B. Donnio and D. Guillon, *Chem.–Eur. J.*, 2002, **8**, 1101; (b) E. Terazzi, S. Torelli, G. Bernardinelli, J.-P. Rivera, J.-M. Benech, C. Bourgogne, B. Donnio, D. Guillon, D. Imbert, J.-C. G. Bünzli, A. Pinto, D. Jeannerat and C. Piguet, *J. Am. Chem. Soc.*, 2005, **127**, 888.

7 B. Dardel, D. Guillon, B. Heinrich and R. Deschenaux, *J. Mater. Chem.*, 2001, **11**, 2814.

8 T. Cardinaels, K. Driesen, T. N. Parac-Vogt, B. Heinrich, C. Bourgogne, D. Guillon, B. Donnio and K. Binnemans, *Chem. Mater.*, 2005, **17**, 6589.

9 S. Campidelli, J. Lenoble, J. Barberá, F. Paolucci, M. Marcaccio, D. Paolucci and R. Deschenaux, *Macromolecules*, 2005, **38**, 7915.

10 H. Nozary, C. Piguet, J.-P. Rivera, P. Tissot, G. Bernardinelli, N. Vulliermet, J. Weber and J.-C. Bünzli, *Inorg. Chem.*, 2000, **39**, 5286.

11 (a) P. Stilbs, *Prog. Nucl. Magn. Reson. Spectrosc.*, 1986, 19; (b) P. S. Pregosin, P. G. A. Kumar and I. Fernandez, *Chem. Rev.*, 2005, **105**, 2977.

12 D. Guillon and A. Skoulios, *Mol. Cryst. Liq. Cryst.*, 1983, **91**, 341.

13 L. Gehringer, C. Bourgogne, D. Guillon and B. Donnio, *J. Am. Chem. Soc.*, 2004, **126**, 3856.

14 B. Donnio and D. Guillon, *Adv. Polym. Sci.*, 2006, DOI: 10.1007/12_079.